http://dx.doi.org/10.5012/bkcs.2012.33.3.1029

Time-Dependent Density Functional Theory Study on Cyclopentadithiophene-Benzothiadiazole-Based Push-Pull-Type Copolymers for New Design of Donor Materials in Bulk Heterojunction Organic Solar Cells†

Jamin Ku,[‡] Daekyun Kim,[‡] Taekhee Ryu,[‡,§] Eunhwan Jung,[‡] Yves Lansac,[#,*] and Yun Hee Jang[‡,*]

[‡]*School of Materials Science and Engineering, Gwangju Institute of Science and Technology, Gwangju 500-712, Korea*
[*]*E-mail: yhjang@gist.ac.kr*
[§]*Supercomputing Center, Korea Institute of Science and Technology Information, Daejeon 305-806, Korea*
[#]*GREMAN, UMR 7347, Université François Rabelais, 37200 Tours, France*
[*]*E-mail: yves.lansac@univ-tours.fr*
Received December 5, 2011, Accepted February 8, 2012

Push-pull-type copolymers – low-band-gap copolymers of electron-rich fused-ring units (such as cyclopentadithiophene; CPDT) and electron-deficient units (such as benzothiadiazole; BT) – are promising donor materials for organic solar cells. Following a design principles proposed in our previous study, we investigate the electronic structure of a series of new CPDTBT derivatives with various electron-withdrawing groups using the time-dependent density functional theory and predict their power conversion efficiency from a newly-developed protocol using the Scharber diagram. Significantly improved efficiencies are expected for derivatives with carbonyl [C=O], carbonothioyl [C=S], dicyano [$C(CN)_2$] and dicyanomethylene [$C=C(CN)_2$] groups, but these polymers with no long alkyl side chain attached to them are likely to be insoluble in most organic solvents and inapplicable to low-cost solution processes. We thus devise several approaches to attach alkyl side chains to these polymers while keeping their high efficiencies.

Key Words : Organic solar cell, Push-pull-type copolymer, Time dependent density functional theory

Introduction

With a possibility of roll-to-roll mass production from low-cost light-weight flexible materials, organic photovoltaics (OPV) is recognized as an emerging technology which has a potential to bring down the cost of solar energy to the level of the conventional fuel costs. OPV can open the door to using solar energy in many interesting applications such as roll-up powers for portable electronics, solar-harvesting fabrics, paints, coatings, and so on. The power conversion efficiency (PCE) is low at the moment, but there has been a dramatic progress in making efficient OPV cells after the introduction of the donor-acceptor bulk heterojunction (BHJ) architecture where polymeric donors are mixed with fullerene-derivative acceptors such as [6,6]-phenyl-C_{61}-butyric acid methyl ester (PCBM).[1-6] The PCE has also significantly leaped after the introduction of push-pull-type alternating copolymeric donors in the BHJ active layer.[7-20] Having both electron-rich units and electron-deficient units, the push-pull-type copolymers exhibit low band gap and strong absorption of the solar spectrum. In the push-pull copolymers used to make the best BHJ OPV cells reported so far,[7-16,18] benzothiadiazole (BT; Figure 1) has been almost exclusively chosen as electron-deficient unit, while electron-rich units have been chosen from various fused rings such as cyclopentadithiophene (CPDT; **1'** in Figure 1).

In our previous studies,[21,22] we have shown that the PCE of PCBM-based BHJ OPV cells containing CPDTBT-like push-pull donor copolymers (including **1**-**3** in Figure 1) can be predicted very well from the electronic structure calculated on the dimer models of the donor polymers (Figure 1) using density functional theory (DFT) and time-dependent DFT (TDDFT) methods at the level of B3LYP/6-311G(d,p). We have also proposed that the PCE could be enhanced by lowering the HOMO/LUMO (highest occupied and lowest unoccupied molecular orbitals) energy levels of the electron-rich unit in such copolymer while keeping the low band gap, which can be achieved by replacing the bridging carbon [$C(alkyl)_2$] in CPDT (**1'** in Figure 1) with an electron-withdrawing group (X in Figure 1). Therefore, in this work we investigate the electronic structure and predict the PCE for a series of derivatives of CPDTBT (**1**) with its bridging carbon group replaced by various electron-withdrawing groups, as an effort to find a newly-designed donor polymer which can be used in high-performance BHJ OPV cells.

First, in Section 3.1, we consider the derivatives **4**-**9** (Figure 1) because their electron-rich components **4'**-**9'**, that is, dialkylmethylene (**4'**), sulfide (**5'**), carbonothioyl (**6'**), carbonyl (**7'**), dicyanomethylene (**8'**), and dicyano (**9'**) derivatives of CPDT **1'**, have been proposed as promising candidates for optoelectronic applications owing to their narrow band gaps and low LUMO levels,[23,24] although the band gaps were significantly overestimated in these DFT (not TDDFT) studies at the level of B3LYP/6-31(d).[23,24]

†This paper is to commemorate Professor Kook Joe Shin's honourable retirement.

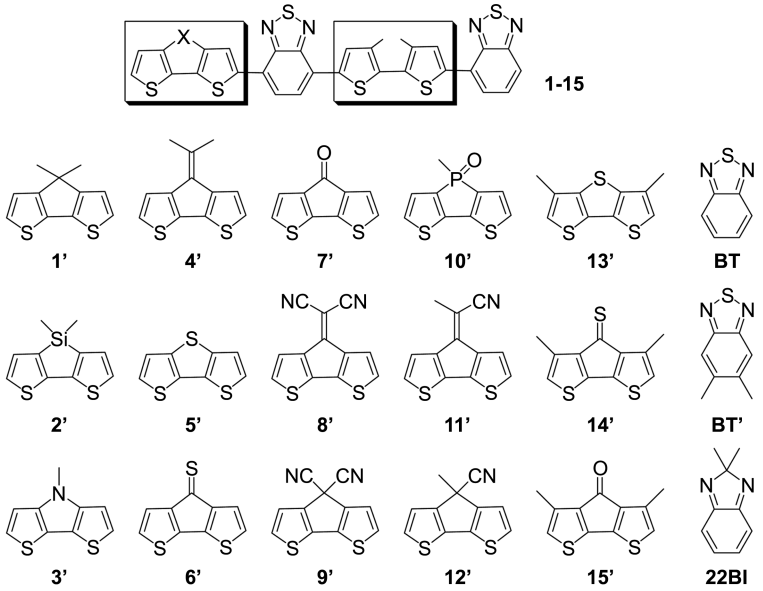

Figure 1. Dimer models of CPDTBT-based copolymers **1-15** (= **1'-15'** + **BT**) and **8BI** (= **8'** + **22BI**), which are considered in this study as an extension of our previous study[21] on **1-3** and **10-12**.

Through a careful comparison with a collection of experimental data, our previous study[21] has shown that the DFT method combined with TDDFT at the level of B3LYP/6-311G(d,p) can reproduce very well the experimental HOMO/LUMO levels and band gaps of such push-pull-type copolymers as long as they are used with a decent size of model (a dimer model), which is encouraging because there has been a doubt on the reliability of the TDDFT method with a conventional functional such as B3LYP in predicting the charge-transfer-type electronic transitions of push-pull-type copolymers. Thus, in the current study, the same DFT/TDDFT approach at the level of B3LYP/6-311(d,p) was used to calculate the electronic structures of **4-9** with a sufficient accuracy for estimating PCE *via* the Scharber diagram, which relates the PCE to the band gap (E_g) and the LUMO energy level (E_{LUMO}) of the constituent donor polymer, based on the insight that the good light absorption (low band gap) and the high open circuit voltage (low HOMO/LUMO levels) are the requisites for good OPV performance.[12,25]

However, the Scharber diagram does not take into account the variation in transition probability of the lowest electronic transitions (HOMO→LUMO) occurring in different donor materials. While this was not a critical problem in our previous study[21] where all the copolymers showed similar transition characteristics, that is, only one strong low-energy transitions in the range of 500-1000 nm (oscillator strength f = 0.7-1.3), some copolymers (**6** and **8**) considered in the current study showed a peculiar transition characteristics, that is, a very week extra peak corresponding the lowest-energy transition at ~950 nm (f < 0.2; See below Figures 4 and 5). Their PCE would be overestimated if only the energy of the lowest transition (that is, the band gap and the LUMO level) is plugged into the Scharber diagram without considering the strength of the transition. Thus, in this work, a new protocol is developed to take into account the transition probability (or oscillator strength calculated with TDDFT) in the PCE estimation. Comparing the PCEs estimated for **1** and for **4-9**, two contributions to the PCE improvement from **1** to **4-9** are clearly distinguished: a negligible contribution from extending π-delocalization through a double bond attached to the fused ring (as in **4**) and a strongly positive contribution from adding an electron-withdrawing group (as in **5-9**). The copolymers **5-9** are expected to show improved PCEs once are incorporated into an OPV cell (See below Table 1).

However, the copolymers **5-9** without long alkyl chains attached to them would be insoluble in organic solvents, and a low-cost solution process for device fabrication would be inapplicable. The alkyl chains are generally introduced to the bridging carbon of the fused rings as in **1-4**, but this site is occupied by the electron-withdrawing group in **5-9**. Thus, in Section 3.2, we introduce one or two alkyl chains (methyl groups in our models) to the copolymers **5-9** in various alternative manners, either to the fused-ring unit or to the BT unit (Figure 1). First, an alkyl chain is introduced to the fused ring either by increasing the valence of the bridging atom of **7** from carbon to phosphorous (**10**) or by replacing one of the two electron-withdrawing groups in **8-9** with it (**11-12**) as considered in our previous study.[21] We also introduce two alkyl chains on the shoulder sites of the fused rings in **5-7** (**13-15**). It is shown that the first approach retains good PCE (**10**) but the others, the last ones in particular (**13-15**), lead to a significant deterioration of PCE, owing to the electron-donating effect of alkyl groups (which lifts upward the HOMO/LUMO levels) in **11-15** and a severe distortion induced by the protruding alkyl groups in **13-15** (See below Table 1 and Figures 2b and 3c). We could also introduce alkyl chains to BT (**BT'** in Figure 1) to increase the solubility of the copolymer, but alkyl chains on

the phenyl ring of BT would have the same negative effect as those on the shoulder sites of **13'-15'**. It would be desirable to develop an electron-deficient unit, that is, an analogues of BT, which can receive alkyl side chains without sacrificing PCE. Indeed, this approach has been employed in a recent development of the best OPV copolymers based on alkylated thienothiophene or thienopyrroledione groups.[17,19,20] Here we increase the valence at the tip of BT by replacing the sulfur atom with a carbon and introduce two alkyl side groups, forming 2,2-alkylbenzimidazole (**22BI**), a quinoid-type isomer of 1,2-alkylbenzimidazole. In fact, Suh and coworkers[26] have recently reported that a BHJ OPV donor copolymer in which the BT unit was replaced by **22BI** showed good solubility at room temperature in various organic solvents while keeping a PCE comparable to the PCE of the BT-based original polymer. Likewise our estimation predicts that the copolymer composed of **8'** and **22BI** (**8BI**) would retain the high PCE of the original BT-based copolymer **8**. With this new electron-deficient unit **22BI**, the design scope of the electron-rich fused-ring unit could be expanded with no need to introduce long alkyl chains at their bridge sites.

Calculation Details

The same type of calculation as carried out for **1-3** and **10-12** in our previous study[21] is used to build the MO energy diagrams of **1-15** and **8BI** to estimate their PCE values. The optimized structure of the dimer model of CBDTBT (**1**) is taken from our previous work[21] and modified to form the dimer models of these derivatives. Geometry optimization of each derivative and its separate units (fused rings, BT, and **22BI**) in the ground state is then carried out at the B3LYP/6-311G(d,p) level of DFT. All the optimized geometries are confirmed to be minimum-energy structures with the normal mode analysis. Some dimer models show an imaginary frequency, but the magnitude of the frequency is negligibly small (< 20 cm^{-1}) and the mode corresponds to an overall deformation of the whole fragment rather than a specific local distortion. For such a mode following an extremely shallow potential energy surface, it would be difficult to locate a minimum-energy point and even doing so would hardly change the calculated electronic structure. Thus, we assume that it is sufficient to take these structures for the electronic structure calculations. The HOMO energy levels (E_{HOMO}) of each derivative are taken from the eigenvalues of the Kohn-Sham equation. The *Jaguar v6.5* software[27,28] is used for these calculations. At the optimized geometry of each copolymer, the singlet-singlet electronic transition energies are calculated using the TDDFT at the same level of B3LYP/6-311G(d,p) to estimate the HOMO-LUMO energy gaps (or band gaps; E_g) and in turn the LUMO energy levels [$E_{LUMO} = E_{HOMO}$ (DFT) + E_g (TDDFT)]. The *Gaussian03* program[29] is employed for these calculations. Absorption spectra are also predicted on the basis of the TDDFT calculations. Gaussian functions with a fixed width of 0.4 eV are employed to build a continuous spectrum from a collection of transition peaks corresponding to the TDDFT transition energies and oscillator strengths (See Figure 5 below). All the calculations are carried out in the gas phase.

Results and Discussion

Improving Electronic Structure: Copolymers 4-9. Figures 2(a) and 3(a)-(b) show the minimum-energy structures and the torsion energy curves as a function of the dihedral angles between the fused ring and BT ($S_{fused}C_{fused}C_{BT}C_{BT}$; θ_{SCCC}) for some representative cases of the copolymers **4-9** (on the monomer models for clear presentations; the dimer models show essentially the same structures and behaviors as shown here). As found for **1-3** in our previous study,[21] the copolymers **4-9** are essentially planar along the polymer backbone in their minimum-energy structures. Their dihedral angles θ_{SCCC} corresponding to the minimum energies are either less than 5° or greater than 175°.

The major (f > 0.15) low-energy (< 3 eV) singlet-singlet electronic transitions calculated at the minimum-energy structures of the copolymers **1-9** are described in Table 1. The transition energy (E_g), the oscillator strength (f), and the energy levels of the MO's involved in the transition are listed. In most cases the lowest-energy transitions from HOMO to LUMO are strong (f = 1.1-1.4), but in the case of **6** and **8** the transition from HOMO to LUMO+2 (f = 0.8-0.9) is stronger than the HOMO-to-LUMO transition (f = 0.1-0.2). They are summarized as MO energy diagrams in Figure 4, and the absorption spectra of **4-9** built from the TDDFT calculations are shown in Figure 5. The spectra clearly show that the transition probability of the low-energy transition varies significantly among different polymers (**6** and **8** in the middle column in Figure 5 *versus* the other copolymers, in particular).

Therefore, we propose a new procedure which can take into account this variation of the transition probability in the Scharber-diagram-based prediction[12,25] of the PCE of PCBM-based BHJ OPV cells containing these donor polymers. First, the PCE_i value is estimated for each low-energy (< 3 eV or > 400 nm) transition (the i-th transition) identified from the TDDFT calculation, by plugging the transition

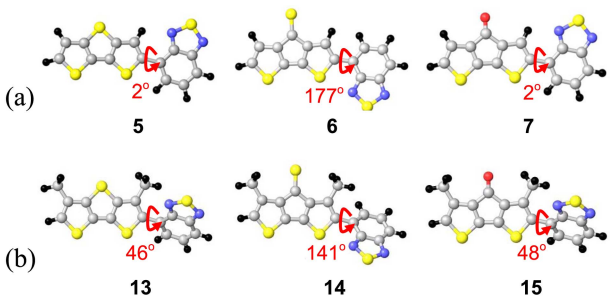

Figure 2. Minimum-energy structures of (a) the copolymers **5-7** and (b) their alkylated derivatives **13-15**, which were optimized at the level of B3LYP/6-311G(d,p) on their dimer models. Only the monomers are shown for clarity. Color dimer code: black (H), gray (C), blue (N), red (O), and yellow (S). The red curved arrow indicates the dihedral angle θ_{SCCC} between the fused ring and BT.

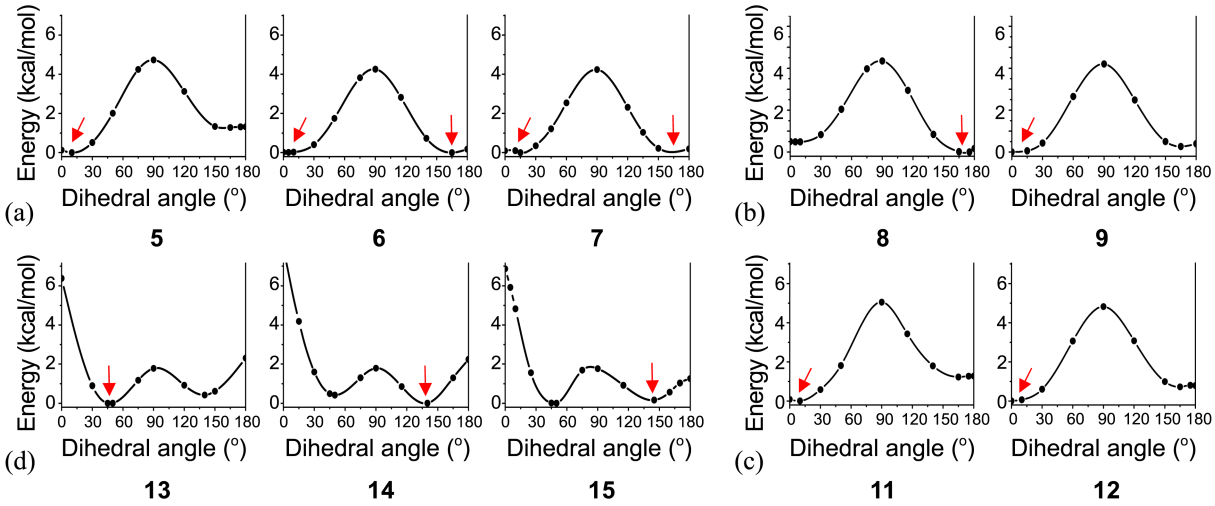

Figure 3. Torsion energy curves along the dihedral angle θ_{SCCC} of (a-b) the copolymers **5-9** and (c-d) their alkylated derivatives **11-15**, which were calculated at the level of B3LYP/6-311G(d,p) on their monomer models. The red arrow indicates the dihedral angle corresponding to the minimum energy.

energy ($E_{g,i}$) and the LUMO level ($E_{LUMO,i}$) into the Scharber diagram,[12,25] as done in our previous study[21] (the seventh column in Table 1). Now the difference is that each PCE_i value is weighted with the oscillator strength (f_i) and these weighted PCE values (f_i·PCE_i) are summed over all the relevant transitions to give the final PCE (PCE = $\Sigma_i f_i$·PCE_i; the ninth column in Table 1).

However, because the oscillator strengths calculated by TDDFT are generally less accurate than the corresponding transition energies, this approach should be used as a tool to estimate the relative, rather than absolute, values of PCE between donor polymers with similar characteristics. Indeed, the PCE's of the compounds **1-3**, which have been estimated as 3.2%, 3.5%, and 2.4% in our previous study[21] in good agreement with experiments, are estimated as 4.0%, 4.3%, and 2.9% with this new procedure (Compare the seventh and

Table 1. Major electronic transitions of the copolymers and the PCE of BHJ OPV cells made of them[a]

	i-th tr	$HOMO_i$ (eV)	$E_{g,i}$ (eV)	$LUMO_i$ (eV)	f_i	PCE_i (%)	$f_i \cdot PCE_i$ (%)	$\Sigma_i f_i \cdot PCE_i$ = PCE(%)	PCE(exp)[b] (%)
1	ex1	−4.93	1.74	−3.20	1.21	~3.2	~3.9	~4	2.6, 3.2~3.5 (5.5~6)
2	ex1	−5.03	1.81	−3.22	1.17	~3.5	~4.1	~4	3.8 (4.7~5.8)
3	ex1	−4.86	1.72	−3.14	1.14	~2.4	~2.7	~3	1.02~2.80
4	ex1	−4.86	1.69	−3.17	1.21	~2.3	~2.8	~3	
5	ex1	−5.28	1.91	−3.37	1.16	~5.6	~6.5	~7	
6	ex1	−5.36	1.27	−4.09	0.15	~11	~1.7	~7	
	ex5	−5.36	1.98	−3.38	0.89	~5.0	~4.4		
7	ex1	−5.38	1.74	−3.64	1.07	~7.0	~7.5	~8	
8	ex1	−5.57	1.32	−4.24	0.20	~13	~2.6	~10	
	ex3	−5.57	1.92	−3.65	0.79	~7.0	~5.5		
9	ex1	−5.73	1.96	−3.77	1.38	~7.5	~10.4	~11	
10	ex1	−5.49	1.92	−3.58	1.29	~6.2	~8.0	~9	
11	ex1	−5.26	1.66	−3.60	0.93	~6.7	~6.2	~7	
	ex3	−5.26	2.09	−3.17	0.18	~3.5	~0.6		
12	ex1	−5.34	1.86	−3.48	1.28	~5.8	~7.4	~8	
13	ex1	−5.41	2.12	−3.28	0.63	~4.0	~2.5	~3	
14	ex1	−5.39	1.44	−3.95	0.09	~10	~0.9	~4	
	ex5	−5.39	2.06	−3.33	0.49	~4.5	~2.2		
15	ex1	−5.31	1.86	−3.45	0.91	~5.5	~5.0	~5	
8BI	ex1	−5.46	1.27	−4.19	0.25	~13	~3.3	~11	
	ex3	−5.46	1.70	−3.76	0.74	~8.0	~5.9		

[a]Estimated from the band gaps (E_g), resulting LUMO levels, and oscillator strengths (f) of the lowest-energy (< 3 eV) singlet-singlet transitions with high oscillator strengths (f > 0.15), using TDDFT calculations on the dimer models and the Scharber diagram.[12,25]. [b]See text in Reference 21 for the review on the references for **1**,[7,8,30] **1** with special treatments (in parentheses),[9,10] **2**,[16,31] **2** with special treatments (in parentheses),[30] and **3**.[32]

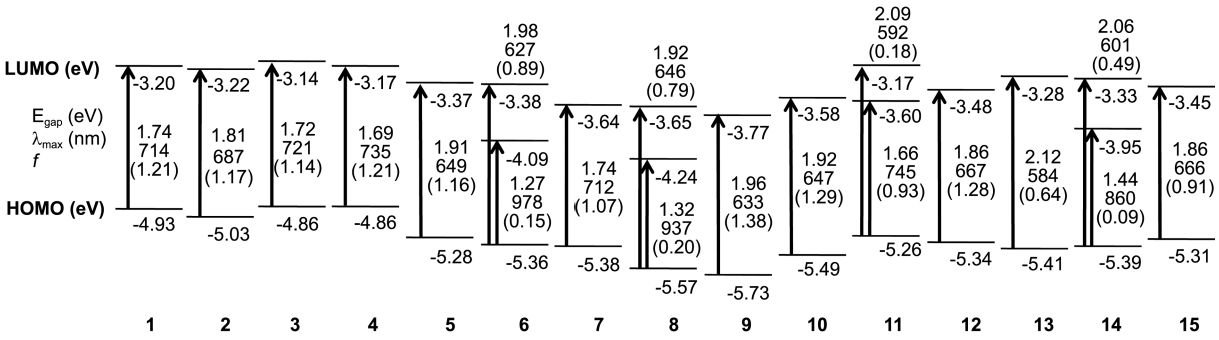

Figure 4. Frontier MO energy diagrams built from DFT/TDDFT [B3LYP/6-311G(d,p)] calculations on the dimer models. The HOMO levels are from DFT, while the band gaps (E_g and λ_{max}) are from TDDFT. The arrows indicate the first singlet-singlet transition (mostly HOMO→LUMO) and other strong (oscillator strength $f > 0.18$) low-energy transitions (mostly HOMO→LUMO+2) of each copolymer. This information is plugged into the Scharber diagram[12,25] to estimate PCE, as summarized in Table 1.

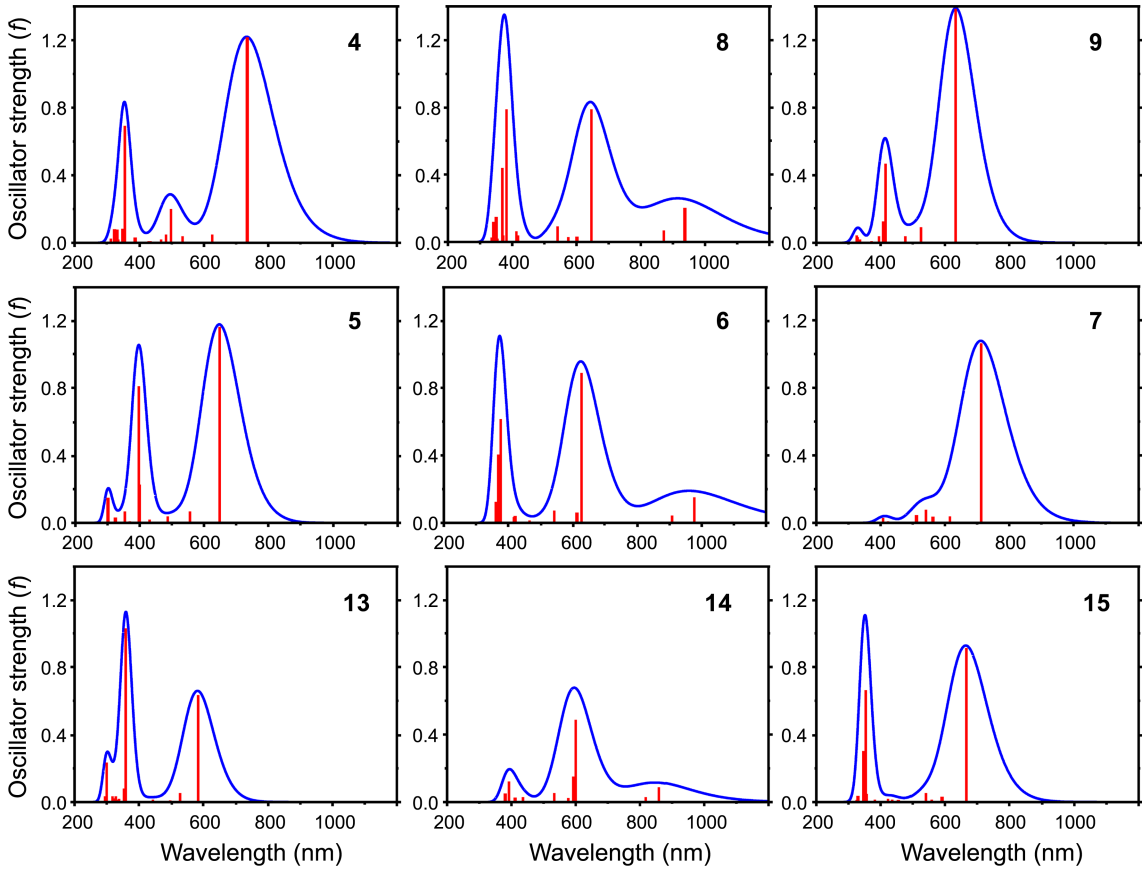

Figure 5. Absorption spectra of representative copolymers (blue curves) built from the TDDFT calculations of transition energies λ_{max} and oscillator strengths *f* (red bars).

the ninth columns in Table 1). Since the compounds **1-3**, as well as **4-9** except **6** and **8**, share similar transition behavior (that is, one strong peak in the range of 500-1000 nm with similar *f* values; Figure 5) with each other, the relative order of PCE (**2** > **1** > **3**) remains the same with or without applying this new procedure. [It is noted that a scale-down of the oscillator strength *f* by 10-20% would bring the current PCE values back to the original values and to the experimental values. The significance of the absolute values of TDDFT oscillator strengths and the sound basis of scaling them down will be further investigated and reported separately in near future.]

On the other hand, the new approach affects a great deal the PCE estimation for **6** and **8**. The copolymers **6** and **8** show two transition peaks in the range of 500-1000 nm, a moderate one ($f \sim 0.8$ and 0.9) at the usual positions of 600-700 nm and another weak one ($f \sim 0.2$) at lower energies (900-1000 nm) (Figure 5). The old approach would estimate their PCE's very high (11% and 13%) owing to their lowest-energy transitions (900-1000 nm) corresponding to very low

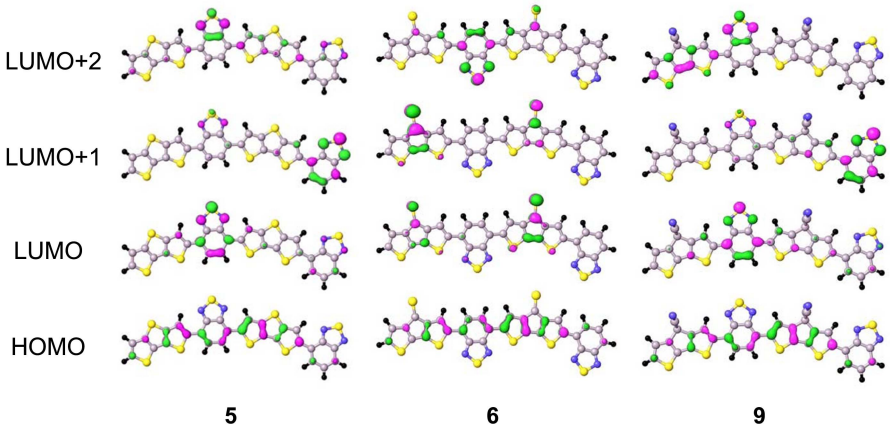

Figure 6. Frontier MO's of some representative copolymers **5**, **6**, and **9** with "aliphatic" (**5** and **9**) and "aromatic" (**6**) electron-withdrawing groups. Color code: gray (C); black (H); yellow (S); blue (N); red (O); pink and light green (different phases of MO).

band gaps (1.27 and 1.32 eV) and low-lying LUMO levels (−4.09 and −4.24 eV), positioning them top-ranked in the series (**8** > **6** > **9** > **7** > **5** > **2** > **1** > **3** > **4**). After the low weighting factors of f (~0.2) are applied through the new approach, their lowest-energy transitions have only minor contributions to PCE. Added up with the major but moderate contributions (f ~ 0.8 and 0.9) from the HOMO-to-LUMO+2 transitions at 1.98 and 1.92 eV (~600 nm), their final PCE values are estimated significantly lower (7.1% for **6** and 9.6% and **8**) with the new protocol. They are dethroned by **9** (11%) and **7** (8.1%) as top-PCE copolymer among the series (**9** > **8** > **7** > **6** > **5** > **2** > **1** > **3** > **4**), while the order of the other copolymers remaines the same (**9** > **7** > **5** > **2** > **1** > **3** > **4**) with both protocols.

The peculiar characteristics of the copolymers **6** and **8** are explained as the following. The copolymer **5**-**9**, all with electron-withdrawing groups, have the HOMO and LUMO levels significantly lower than those of **1** (Figure 4), but their MO characteristics show a clear difference between two copolymer groups, the ones that have electron-withdrawing groups participating in the π-delocalization extended *via* a double bond, that is, "aromatic electron-withdrawing groups" (**6** and **8**) and the others which have a simple attachment of the electron-withdrawing groups (**5**, **7**, and **9**). See Figure 6 for the examples of **5**, **6**, and **9**.

As shown in Figure 6 for **5** and **9**, the copolymers **5**, **7**, and **9** share the MO characteristics of **1**, which have been shown in our previous study:[21] (1) the HOMO-1 of each copolymer unit mostly comes from the HOMO of the fused-ring unit (which is higher than the HOMO of BT); (2) the HOMO level comes from the hybridization of the HOMO of the fused-ring unit and the HOMO of BT; (3) the LUMO and LUMO+1 levels come from the LUMO of the BT unit (which is lower than the LUMO of the fused ring) as the in-phase and out-of-phase combination, respectively. The lowest-energy transition, which is quite strong (f > 1), mostly involves an intramolecular charge transfer from a π-orbital delocalized over all the units (HOMO) to an orbital mostly localized on the BT unit (LUMO). The transition energy varies between 1.60 and 1.96 eV. [This charge-transfer character has led to a concern on the reliability of the TDDFT method with a conventional functional such as B3LYP in describing the electronic transitions of push-pull-type polymers, but our previous study,[21] through a careful comparison with a collection of experimental data, showed that the TDDFT at the level of B3LYP/6-311G(d,p) are quantitatively accurate as long as they are used with a decent size of models of such polymers.

As also shown for **6** in Figure 6, the copolymers **6** and **8** share the same HOMO characteristics but NOT the same LUMO characteristics as the other class of copolymers. The C=S and C=C(CN)$_2$ "aromatic electron-withdrawing" groups attached to their fused-ring units induces a great deal of downward shift of their MO's, the LUMO in particular. The LUMO levels of **6'** and **8'** (−4.20 and −4.41 eV) are significantly lower than those of **1'** (CPDT; −1.55 eV), **9'** ("aliphatic" counterpart of **8'** with C(CN)$_2$; −2.52 eV), and even the BT unit (−2.97 eV). As a result, the LUMO and the LUMO+1 of the copolymers **6** and **8** come from the LUMO of the fused-ring units, and the LUMO+2 comes from the LUMO of the BT unit. That is, the BT-localized characteristics of the LUMO of most of the copolymers (**1**-**5**, **7**, and **9**) is shared by the LUMO+2, rather than by the LUMO, of the copolymers **6** and **8**. This explains the weak HOMO-to-LUMO and the strong HOMO-to-LUMO+2 transitions of **6** and **8**.

Summarizing, the PCE values estimated for **6** and **8** with the new protocol (7.1% and 9.6%) are similar to (or even lower than) the values estimated for their "aliphatic" analogues **5** and **9** (6.8% and 11%). In fact, the copolymer **4**, the "aromatic" counterpart of **1** without any electron-withdrawing group, has a slightly lower band gap (1.69 eV) than **1** (1.74 eV) owing to the π-delocalization extended over to the methylene group, but its higher LUMO level and lower oscillator strength lead to the lowest PCE (2.9%) among the series of **1**-**9**. It appears that, while adding electron-withdrawing groups to the fused ring improves the PCE, adding an aromatic nature to the electron-withdrawing group has only a negligible (or even a negative) effect: **9** > **8** > **7** > **6** ≈ **5** > **2** > **1** > **3** > **4**.

Improving Solubility by Adding Alkyl Chains: Copolymers 10-15 and 8BI. To increase the solution processability of the promising copolymers **5-9**, we devised several approaches to attach alkyl (methyl groups in our models) side chains to them while keeping their electron-withdrawing groups. First, an alkyl chain per monomer unit is introduced to the bridging site in the fused ring of **7** after increasing its valence by replacing the carbon atom to phosphorous; **10**) or to the fused ring of **8-9** by replacing one of the two electron-withdrawing groups with it (**11-12**) (Figure 1). We note a significant deterioration of PCE from **8-9** (9.6% and 11%) to **11-12** (7.4% and 7.7%), which should originate from the electron-donating effect of alkyl groups lifting upward the HOMO/LUMO levels. On the other hand, the first approach slightly improves PCE from **7** (8.1%) to **10** (8.7%) mostly due to the increase of the oscillator strength (See Table 1). Those effects are rather electronic than structural, because the alkyl chains introduced in both approaches do not perturb the planar conformation of the polymer backbone. The dihedral angle θ_{SCCC} is less than 5° in the minimum-energy structures of **10-12**, and the torsion energy curves of **10-12** show the same feature as those of **1-9** (See Figures 3(c)). In fact, these derivatives **10-12** have been considered in our previous study.[21] Using the old protocol, we have predicted their PCE values as 6.2%, 6.7%, and 5.8%, which have been significantly improved from the value for **1** (3.2%), and suggested the copolymer **11** as the most promising candidate (**11** > **10** > **12**).[21] The new protocol in the current work predicts rather different (overestimated) PCE's for **10-12** (8.7%, 7.4%, and 7.7%). The copolymer **11**, a mono-alkyl derivative of **8**, shares the peculiar transition characteristics with **8** (Figure 4), and the new protocol places the PCE of **11** behind the others (**10** > **12** > **11**) as it did to **6** and **8** in the previous section. In any case, it is still valid that all of the copolymers **10-12** can be promising candidates with PCE's significantly improved from the PCE of **1** (4.0%).

On the other hand, when two alkyl chains per monomer unit are introduced to the shoulder sites in the fused rings of **5-7** to form new derivatives **13-15** (Figure 1), the fused ring and BT are significantly twisted from each other in the minimum-energy structures (θ_{SCCC} ~ 50° or 145°; Figures 2(b) and 3(d)) because of the steric hindrance between the alkyl groups and BT. As a result, the π-delocalization along the polymer backbone is disrupted, the band gap increases (from 1.91, 1.27, and 1.74 eV of **5-7** to 2.12, 1.44, and 1.86 eV of **13-15**), the LUMO level goes upwards, and the oscillator strength is reduced (Table 1 and Figures 4; Compare **5-7** and **13-15** in Figure 5). All these effects, in addition to the electron-donating effect of alkyl groups, led to a significant deterioration of PCE from 7-8% of **5-7** to 3-5% of **13-15**. Expecting the same negative effect, we skip introducing alkyl chains to the phenyl ring of BT as in **BT'** (Figure 1).

Instead we devise an analogue of BT which could receive alkyl side chains without inducing steric hindrance to neighboring units. We replace the sulfur atom at the tip of BT with an sp^3 carbon atom. The resulting **22BI** (Figure 1) is expected to be a promising electron-deficient unit (as proven by Suh and coworkers[26]), because its LUMO level (−3.09 eV) is comparable to and even slightly lower than that of BT (−2.97 eV) while its HOMO (−6.49 eV) is placed much higher than that of BT (−6.84 eV). Indeed, when we connect **8'** and **22BI**, the resulting **8BI** copolymer retains the planar conformation over the backbone as well as low band gap [1.32 (**8**) *versus* 1.27 (**8BI**) eV] and deep LUMO level [−4.24 (**8**) *versus* −4.19 (**8BI**) eV]. This new copolymer **8BI** is predicted to show a PCE of 11%, comparable to the original BT-based copolymer **8**. Thus, we propose that the combination of a fused ring introduced with an electron-withdrawing group (such as **5-9**) and a BT analog incorporated with alkyl side chains (such as **22BI**) as a promising approach to develop low-cost high-performance BHJ OVP donor polymers, as long as they also meet other requirements including favorable morphology and charge transport properties as well as stability. A more detailed study along this line is in progress and will be reported separately.

Summary

Following the design principles proposed in our previous study,[21] a TDDFT study was carried out on a series of cyclopentadithiophene-benzothiadiazole (CPDTBT)-based copolymers with various electron-withdrawing groups on the fused-ring (CPDT) unit to investigate their electronic structure and to predict their PCE values from a newly-developed protocol using the Scharber diagram. High PCE values were expected for derivatives with sulfide (**5**), carbonothioyl (**6**), carbonyl (**7**), dicyanomethylene (**8**), and dicyano (**9**) groups, but these polymers with no long alkyl side chain attached to them are likely to be insoluble in most organic solvents and inapplicable to low-cost solution processes. We thus devised several approaches (**10-12** and **8BI**) to attach alkyl side chains to these polymers while keeping their high efficiencies. A particularly promising approach is that we add two alkyl chains to the BT unit (rather than the fused-ring unit) after increasing the valence of the tip by replacing the sulfur atom to $C(alkyl)_2$. This new 2,2-dialkyl-benzimidazole (**22BI**) electron-deficient unit, which has recently been successfully incorporated to a BHJ OPV donor polymer,[26] will be considered in more detail in our separate study in near future. Obviously, the best-fit electronic structure of donor polymers may not necessarily guarantee the best solar cell efficiency. A multi-scale modeling approach combining quantum mechanics and molecular dynamics calculation is in progress to understand and predict other relevant characteristics of these polymers, such as the nanometer-scale morphology in the mixture of polymer:fullerene BHJ active layer and the charge transport through it.

Acknowledgments. This work was supported by NRF (*via* the Basic Research program, the International Collaboration program, the National Research Laboratory program, and the Scientist Exchange Program), by GIST (PIMS and

SCENT), and by KISTI (through the Grand Challenge and Creative Challenge programs and the PLSI supercomputing resources).

References

1. Yu, G.; Gao, J.; Hummelen, J. C.; Wudl, F.; Heeger, A. J. *Science* **1995**, *270*, 1789.
2. Ma, W.; Yang, C.; Gong, X.; Lee, K.; Heeger, A. J. *Adv. Funct. Mater.* **2005**, *15*, 1617.
3. Li, G.; Shrotriya, V.; Huang, J.; Yao, Y.; Moriarty, T.; Emery, K.; Yang, Y. *Nature Mater.* **2005**, *4*, 864.
4. Thompson, B. C.; Frechet, J. M. J. *Angew. Chem. Int. Ed.* **2008**, *47*, 58.
5. Cheng, Y.-J.; Yang, S.-H.; Hsu, C.-S. *Chem. Rev.* **2009**, *109*, 5868.
6. Dennler, G.; Scharber, M. C.; Brabec, C. J. *Adv. Mater.* **2009**, *21*, 1323.
7. Muhlbacher, D.; Scharber, M.; Morana, M.; Zhu, Z.; Waller, D.; Gaudiana, R.; Brabec, C. *Adv. Mater.* **2006**, *18*, 2884.
8. Zhu, Z.; Waller, D.; Gaudiana, R.; Morana, M.; Muhlbacher, D.; Scharber, M.; Brabec, C. *Macromolecules* **2007**, *40*, 1981.
9. Kim, J. Y.; Lee, K.; Coates, N. E.; Moses, D.; Nguyen, T.-Q.; Dante, M.; Heeger, A. J. *Science* **2007**, *317*, 222.
10. Peet, J.; Kim, J. Y.; Coates, N. E.; Ma, W. L.; Moses, D.; Heeger, A. J.; Bazan, G. C. *Nature Mater.* **2007**, *6*, 497.
11. Blouin, N.; Michaud, A.; Leclerc, M. *Adv. Mater.* **2007**, *19*, 2295.
12. Blouin, N.; Michaud, A.; Gendron, D.; Wakim, S.; Blair, E.; Neagu-Plesu, R.; Belletete, M.; Durocher, G.; Tao, Y.; Leclerc, M. *J. Am. Chem. Soc.* **2008**, *130*, 732.
13. Park, S. H.; Roy, A.; Beaupre, S.; Cho, S.; Coates, N.; Moon, J. S.; Moses, D.; Leclerc, M.; Lee, K.; Heeger, A. J. *Nature Photonics* **2009**, *3*, 297.
14. Wang, E.; Wang, L.; Lan, L.; Luo, C.; Zhuang, W.; Peng, J.; Cao, Y. *Appl. Phys. Lett.* **2008**, *92*, 033307.
15. Hellstrom, S.; Zhang, F.; Inganas, O.; Andersson, M. R. *Dalton Trans.* **2009**, 10032.
16. Hou, J.; Chen, H.-Y.; Zhang, S.; Li, G.; Yang, Y. *J. Am. Chem. Soc.* **2008**, *130*, 16144-16145.
17. Chen, H.-Y.; Hou, J.; Zhang, S.; Liang, Y.; Yang, G.; Yang, Y.; Yu, L.; Wu, Y.; Li, G. *Nat. Photonics* **2009**, *3*, 649.
18. Huo, L.; Hou, J.; Zhang, S.; Chen, H.-Y.; Yang, Y. *Angew. Chem. Int. Ed.* **2010**, *49*, 1500.
19. Liang, Y.; Xu, Z.; Xia, J.; Tsai, S.-T.; Wu, Y.; Li, G.; Ray, C.; Yu, L. *Adv. Mater.* **2010**, *22*, E135.
20. Zou, Y.; Najari, A.; Berrouard, P.; Beaupre, S.; Aich, B. R.; Tao, Y.; Leclerc, M. *J. Am. Chem. Soc.* **2010**, *132*, 5330.
21. Ku, J.; Lansac, Y.; Jang, Y. H. *J. Phys. Chem. C* **2011**, *115*, 21508.
22. Abdo, N. I.; Ku, J.; El-Shehawy, A. A.; Min, J.-K.; El-Barbary, A. A.; Jang, Y. H.; Lee, J.-S. *to be submitted*.
23. Salzner, U.; Lagowski, J. B.; Pickup, P. G.; Poirier, R. A. *J. Org. Chem.* **1999**, *64*, 7419.
24. Bouzzine, S. M.; Makayssi, A.; Hamidi, M.; Bouachrine, M. *J. Mol. Struct.: THEOCHEM* **2008**, *851*, 254.
25. Scharber, M. C.; Muhlbacher, D.; Koppe, M.; Denk, P.; Waldauf, C.; Heeger, A. J.; Brabec, C. J. *Adv. Mater.* **2006**, *18*, 789.
26. Song, S.; Jin, Y.; Park, S. H.; Cho, S.; Kim, I.; Lee, K.; Heeger, A. J.; Suh, H. *J. Mater. Chem.* **2010**, *20*, 6517.
27. *Jaguar*, version 6.5; Schrodinger, LLC: New York, NY, 2005.
28. Greeley, B. H.; Russo, T. V.; Mainz, D. T.; Friesner, R. A.; Langlois, J.-M.; Goddard, W. A., III; Donnelly, R. E., Jr.; Ringalda, M. N. *J. Chem. Phys.* **1994**, *101*, 4028.
29. Frisch, M. J.; Trucks, G. W.; Schlegel, H. B.; Scuseria, G. E.; Robb, M. A.; Cheeseman, F. R.; Montgomery, J. A. F.; Vreven, T.; Kudin, K. N.; Burant, J. C.; Millam, F. M.; Iyengar, S. S.; Tomasi, F.; Barone, V.; Mennucci, B.; Cossi, M.; Scalmani, G.; Rega, N.; Petersson, G. A.; Nakatsufi, G.; Hada, M.; Ehara, M.; Toyota, K.; Fukuda, R.; Hasegawa, J.; Ishida, M.; Nakajima, T.; Honda, Y.; Kitao, O.; Nakai, G.; Klene, M.; Li, X.; Know, J. E.; Hratchian, G. P.; Cross, J. B.; Bakken, V.; Adamo, C.; Jaramillo, F.; Gomperts, R.; Stratmann, R. E.; Yazyev, O.; Austin, A. J.; Cmmi, R.; Pomelli, C.; Ochterski, J. W.; Ayala, P. Y.; Morokuma, K.; Voth, G. A.; Salvador, P.; Dnnenberg, J. J.; Zakrzewski, V. G.; Dapprich, S.; Daniels, A. D.; Strain, M. C.; Farkas, O.; Malick, D. K.; Rabuck, A. D.; K., R.; Foresman, J. B.; Ortiz, J. V.; Cui, Q.; Baboul, A. G.; Clifoord, S.; Coislowski, J.; Stefanov, B. B.; Liu, G.; liashenko, A.; Piskorz, P.; Komaromi, I.; Martin, R. L.; Fox, D. J.; Keith, T.; Al-Laham, M. A.; Peng, C. Y.; Nanayakkara, A.; Challacombe, M.; Gill, P. M. W.; Jognson, B.; Chen, W.; Wong, M. W.; Gonzalez, C.; Pople, J. A. *Gaussian 03*, Revision C.02; Gaussian, Inc.: Wallingford, CT, 2004.
30. Coffin, R. C.; Peet, J.; Rogers, J. T.; Bazan, G. C. *Nature Chem.* **2009**, *1*, 657.
31. Chen, H.-Y.; Hou, J.; Hayden, A. E.; Yang, H.; Houk, K. N.; Yang, Y. *Adv. Mater.* **2010**, *22*, 371.
32. Yue, W.; Zhao, Y.; Shao, S.; Tian, H.; Xie, Z.; Geng, Y.; Wang, F. *J. Mater. Chem.* **2009**, *19*, 2199.